

Big shells, bigger data: cohort analysis of Chesapeake Bay *Crassostrea virginica* reefs

Madison D. Griffin^{1,*} Grace S. Chiu^{1,2,3,4,5}
 Roger L. Mann¹ Melissa J. Southworth¹
 John K. Thomas¹

¹William & Mary’s Batten School of Coastal & Marine Sciences & Virginia Institute of Marine Science

²Computational & Applied Mathematics & Statistics (CAMS), College of William & Mary

³Department of Statistical Sciences and Operations Research, Virginia Commonwealth University

⁴Department of Statistics and Actuarial Science, University of Waterloo

⁵Department of Statistics, University of Washington

*Corresponding author: mdgriffin@vims.edu

Abstract

Oysters in Virginia Chesapeake Bay oyster reefs are “age-truncated”, possibly due to a combination of historical overfishing, disease epizootics, environmental degradation, and climate change. Research has suggested that oysters exhibit resilience to environmental stressors; however, that evidence is based on the current limited understanding of oyster lifespan. Until this paper, the Virginia Oyster Stock Assessment and Replenishment Archive (VOSARA), a spatially and temporally expansive dataset (222 reefs across 2003-2023) of shell lengths (SL, mm), had yet to be examined comprehensively in the context of resilience. We develop a novel method using Gaussian mixture modeling (GMM) to identify the age groups in each reef using yearly SL data and then link those age groups over time to identify cohorts and estimate their lifespan. Sixty-four reefs (29%) are deemed to have sufficient data (at least 300 oysters sampled for a minimum of 8 consecutive years) for this analysis. We fit univariate GMMs for each year (t) and reef (r) for each of the seven river strata (R) to estimate 1) the mean and standard deviation of SL for each $a_{Rr,t}$ th age group, and 2) the mixture percentage of each $a_{Rr,t}$ th age group. We link age groups across time to infer age cohorts by developing a mechanistic algorithm that prevents the shrinking of shell length when an $a_{Rr,t}$ th group becomes an $(a_{R,r,t} + 1)$ th group. Our method

shows promise in identifying oyster cohorts and estimating lifespan solely using SL data. Our results show signals of resiliency in almost all river systems: oyster cohorts live longer and grow larger in the mid-to-late 2010s compared to the early 2000s.

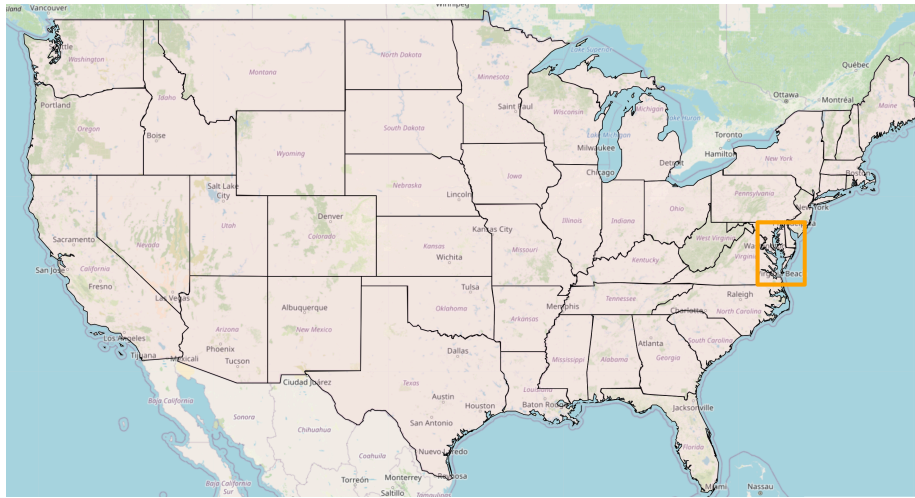
Keywords

Resiliency, Gaussian mixture modeling, age cohorts

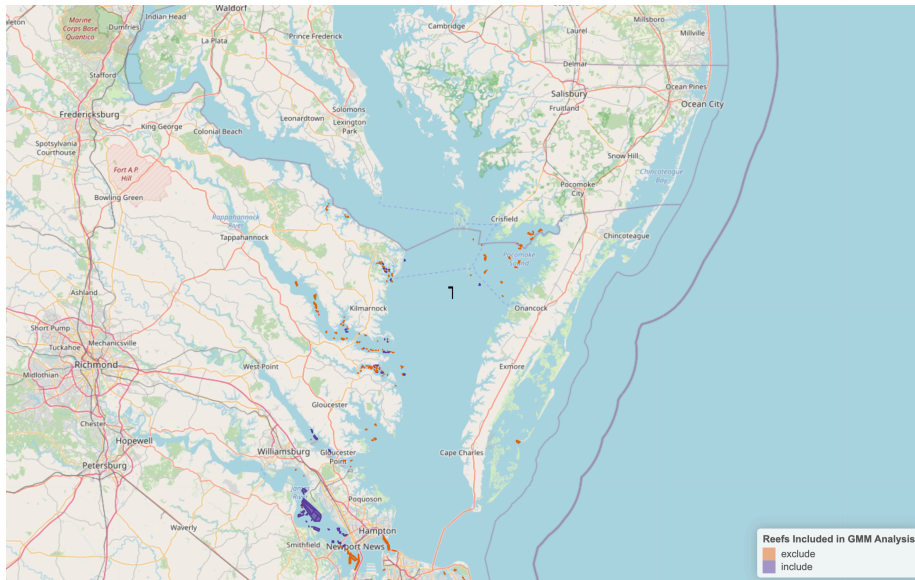
1 Introduction

1.1 Historic declines in oyster populations

The eastern oyster (*Crassostrea virginica*) has played an important ecological, and cultural role in the Chesapeake Bay in the eastern United States (Figure 1a) and its estuaries for over 10,000 years (Mann et al., 2009). Our study only considers the Virginia portion of Chesapeake Bay (Figure 1b). Eastern oyster reefs in the Chesapeake Bay operate within a highly dynamic system, characterized by numerous daily, weekly, and seasonal cycles, all of which are reflected in their shell growth (Baird & Ulanowicz, 1989; Haas, 1977; Pritchard, 1952). Oyster reefs are essential fish habitats, ecosystem engineers, filter feeders, and on average, provide an estimated \$10,000 to \$99,000 per hectare in value from ecosystem services (Coen et al., 1999; Grabowski et al., 2012; Pace et al., 2020). As ecosystem engineers, oyster reefs need to be self sustaining, requiring oysters to live long, die at big sizes, and have ample shell substrate for recruits to settle (Harding et al., 2010; Hemeon et al., 2020; Pace et al., 2020; Solinger et al., 2022).



(a) Map of the contiguous United States. The Chesapeake Bay estuary is situated in the orange box.



(b) The map shows the reefs in the Virginia portion of Chesapeake Bay (VACB) monitored by VOSARA. Reefs in purple ($n = 64$) are included in the cohort analysis, meaning for at least 8 consecutive years there were at least 300 oysters sampled. Reefs included in this study are located in every main VACB tributary except Lynnhaven Bay.

Figure 1: A map of the study location and spatial scale.

The Virginia oyster fishery peaked in the late 1800s; however, fishery output varied from the 1880s through the 1910s (Schulte, 2017). The public oyster replenishment program began in 1929 to address losses in productivity (Schulte, 2017). By the late 1940s, *Perkinsus marinus*, a parasite known as Dermo, caused

annual mortality ranging from 10-30% of market oysters (Schulte, 2017). In the late 1950s, *Haplosporidium nelsoni* (MSX) disease caused large mortality events in Chesapeake Bay (90-95%), which led to major declines in oyster production (Haven & Whitcomb, 1986; Mann & Powell, 2007; Schulte, 2017). Both diseases are still a prominent issue today. This series of epizootics depressed the fishery in the 1980s through 1990s (Schulte, 2017). Conservative management and sustained replenishment efforts by the Virginia Marine Resource Commission resulted in gradual gains through the early 2000's with a sustained improvement in stocks noted in the 2006-2010 period, and continuing growth since that time.

Oyster populations are successful at high densities due to the life history strategy of accumulating into three dimensional reefs (Hemeon et al., 2020; Schulte, 2017). As such, oyster reefs require ample suitable oyster bottom and shell to aid in recruitment and post-settlement success (Hemeon et al., 2020). Oyster death is what supplies shell to the reef (Pace et al., 2020). When shell is lost, due to either fishing mortality or short-half life of oyster shell, recruitment decreases, which decreases the amount of adult oysters, further decreasing shell addition (Pace et al., 2020; Powell et al., 2012). This negative feedback loop is found in many oyster reefs in estuarine environments, hence, net shell loss is greater than net shell gain (Mann et al., 2009; Pace et al., 2020; Powell et al., 2006; Powell et al., 2012; Southworth et al., 2010). Therefore, habitat (*i.e.*, other oysters, both living and dead) are essential for reef sustainability and should be properly managed (Mann & Powell, 2007; Solinger et al., 2022). One method of doing so is to estimate the age structure (*i.e.*, identify age classes and estimate their age) of oyster reefs, and simulate management reference points based on shell accretion and age classes (Solinger et al., 2022). A reef with multiple age classes alive and growing simultaneously are more suitable for rebuilding populations and improving self-sustainability (Mann & Powell, 2007).

The longevity of recruited individuals is essential to effectively rebuild native populations for the benefit of ecological restoration (Mann & Powell, 2007). Older oysters add more shell to a reef due to their bigger size, which is crucial for maintaining reef structure (Mann et al., 2022; Mann & Powell, 2007). However, research suggests that the Chesapeake Bay oyster population is age-truncated, meaning that the proportion of older age classes is low (Harding et al., 2010; Mann et al., 2009; Southworth et al., 2010). Age-truncation has been apparent since the colonial time period. In a study using size to approximate age, oysters were significantly larger in the middle Pleistocene (maximum of 260 mm) compared to colonial oysters (maximum of 124 mm), suggesting that even colonial oysters, often considered the baseline state for the eastern oyster population, were missing older age groups (Kusnerik et al., 2018). At the modern time scale, despite consistently high recruitment events, high mortality between year 0 and year 1 continues to truncate Chesapeake Bay's oyster population, hindering restoration and rebuilding efforts (Mann et al., 2009). For example, in the Piankatank and Great Wicomico Rivers, even though recruitment was high, there were small percentages of age 3+ oysters leading up to the year 2010 (Harding et al., 2010; Southworth et al., 2010). Due to the age-truncation in

Chesapeake Bay oysters, dating back to the colonial period, widely used age-based models in fisheries science (*e.g.*, von Bertalanffy (1938)) are ineffective, requiring innovative approaches using size data (Mann et al., 2022).

1.2 Statistical methods for aging oysters

Researchers have been interested in estimating the age and identifying multi-year cohorts of oysters in Chesapeake Bay; however, few have used a rigorous modeling approach. In the 1954 Annual Report of the Commission of Fisheries of Virginia (Commission of Fisheries of Virginia, 1954), the condition of public oyster grounds was shown to have improved due to the tracking of spat to yearling oysters in the James and Rappahannock rivers. However, this conclusion was reached from simple visualizations of bar charts. By the 2010s, research using the Virginia Oyster Stock Assessment and Replenishment Archive (VOSARA) dataset (Harding et al., 2010; Mann et al., 2009; Southworth et al., 2010) used the Bhattacharya method (Bhattacharya, 1967) to estimate age classes and growth rate in the Piankatank, James, and Great Wicomico Rivers. By producing frequency histograms of shell lengths for each year, the Bhattacharya method identifies clusters of shell lengths using cubic approximations of density for each histogram, allowing the researchers to identify age classes by regarding each cluster as an age class from that year. Though more rigorous than the methods using in the 1950s, this method still relies more heavily on the modeler’s decision making rather than on statistical principles. Further, studies in the 2010s were focused on one river system, rather than holistic approaches to analyze age structure across Chesapeake Bay. Mann et al. (2022) used the TropFishR package (Mildenberger et al., 2017) to identify year classes, then applied Bhattacharya methods to overlay a growth curve on the estimated year classes to calculate mortality rates on a larger scale (regional aggregations of Chesapeake Bay river systems in Virginia and Maryland).

Alongside the ecological research community, the statistical community has worked to improve methods to estimate age groups from length data (Macdonald & Pitcher, 1979). Knowing that this is a common research goal in fisheries science, Macdonald & Pitcher (1979) developed a computer program that transitioned the field from graphical interpretations to model-based approaches by fitting a “distribution mixture”. This method builds off the work of Bhattacharya (1967), improving reproducibility by reducing the amount of interpretation left to the user (which can be biased) (Macdonald & Pitcher, 1979). One such approach is Gaussian mixture modeling (GMM). This method has been used in ecological studies (Fabri-Ruiz et al., 2020; Weise et al., 2022) and fisheries science to estimate age groups (Laslett et al., 2004; Sethi et al., 2017; Shaw et al., 2021; Zhou et al., 2020) based on animal size measurements.

A mixture modeling approach has not been comprehensively applied to the VOSARA dataset. We propose a novel algorithm that applies GMM to the VOSARA dataset to effectively allocate individual oysters (observed from each oyster reef taken from each river stratum) into one of several age groups (Gaus-

sian components) based on the animal’s shell length (SL, mm). Our algorithm also links age groups over time to form cohorts. This unique approach is the first holistic and rigorous analysis of age structure in Virginia’s portion of Chesapeake Bay (VACB), providing insights into the terminal age of oyster cohorts in all the main river systems, and filling a knowledge gap in oyster restoration approaches (Mann & Powell, 2007). Further, this analysis also suggests signals of resiliency of VACB oyster reefs.

A novel GMM approach is needed for the VOSARA data for the following reasons. Our objective is complex: we want holistic insights at the bay-level that encapsulate river- and reef-level characteristics, while using annual animal-level data that span two decades. Other studies on age structure involved less complexity or employed additional validation data that we lack. For example, Shaw et al. (2021) used GMM to estimate age groups of the krill species *Euphausia pacifica*, and were able to link age groups over time to identify cohorts. However, their study area was confined to a small region off the coast of Newport, Oregon, with frequent sampling intervals (median of 16 days), that allowed close monitoring of krill growth. In contrast, our VOSARA dataset is much more spatially (222 reefs) and temporally expansive (21 years), and the sampling interval is approximately annual. Further, most applications of GMM on size data have been used to assess how accurate the method is compared to traditional aging methods, such as scaling of salmonids in Sethi et al. (2017), or against data on fish with known ages and sizes (Zhou et al., 2020). No existing oyster aging method is feasible to validate the “true” ages of each individual oyster at the spatiotemporal scale of VOSARA. Another major distinction between our study and previous applications of GMM is that oysters create their own environment and are immobile once settled (Bonar et al., 1990). Therefore, it is reasonable for our method to assume that oysters still alive in continuing years *are* part of the same cohort, because the only way to move is through natural mortality or fishing mortality.

The rest of this paper is structured as follows. In Section 2, we briefly describe the methodology of the Virginia patent tong survey and the included data. In Section 3, we describe the framework of our methodology to estimate the age structure of oyster reefs in Virginia’s Chesapeake Bay. This section includes the application of GMM to live oysters and a detailed description of our algorithm. In Section 4, we describe the algorithm output, highlighting exemplary results from the Chesapeake Bay mainstem and James river. In Section 5, we discuss the signals of resiliency embedded in the estimated age structure of oysters in oyster reefs located in the Chesapeake Bay Mainstem and James River. In Section 6, we revisit the utility and novelty of our framework and implications of resiliency of eastern oysters in VACB. In Section 7, we conclude by summarizing the results of the method and its potential for future use in management. Supplementary results from the remaining river strata are included in the appendix.

2 Data description

The VOSARA data used for this study are from quantitative fishery independent survey data of 222 natural public oyster reefs in the Virginia tributaries of Chesapeake Bay (Baylor, 1895). This is a collaborative effort between the Virginia Institute of Marine Science (VIMS) and the Virginia Marine Resources Commission (VMRC). A quantitative sampling program using a stratified random grid is used at all selected reefs (Mann et al., 2009; Southworth et al., 2010). Oysters are collected from a hydraulic patent tong that samples one square meter of bottom. The sampling scheme is described in more detail in Southworth et al. (2010). Our analysis used SL data for spat and live oysters from the years 2003 to 2023 (Southworth et al., 2010). Spat oysters are defined as sampled oysters that are alive but do not have a cupped appearance. Live oysters are defined as all other sampled oysters that are alive.

Data from the Nansemond River, Elizabeth River Western Branch, Lafayette River, and Elizabeth River were excluded because they are sampled every other year. The remaining sampled regions were reorganized to match harvest management units set by the VMRC, which we refer to as “river strata”. To reduce uncertainty due to data gaps, we excluded from reef-level analyses those reefs that did not have at least 300 oysters sampled per year over eight consecutive years or more (but all reefs were included in stratum-level analyses). Under these criteria, we conducted reef-level analyses on 64 reefs ($n = 1,205,165$ oysters across 29% of VACB natural, public, oyster reefs). These 64 reefs covered every tributary except Lynnhaven Bay (Figure 1b). The river strata and the 64 included reefs are listed in Table 1.

Table 1: List of (R, r) th river-reef strata combinations and timeframe included in our analysis, depicted in Figure 1b.

River (R)	Reef Name	Reef ID (r)	Years (t)
Chesapeake Bay Mainstem	DEEP ROCK	357	2003-2023
	BLACKBERRY HANG	312	2006-2009, 2011-2023
Great Wicomico River	HAYNIE POINT	64	2003, 2006-2023
	SANDY POINT	133	2003-2023
	SHELL BAR	135	2003-2004, 2006-2023
	ROGUE POINT	187	2003-2023
	HARCUM FLATS	409	2003-2004, 2006-2023
	COE 11	1311	2006-2023

River (R)	Reef Name	Reef ID (r)	Years (t)
James River	COE 13	1313	2005-2009, 2011-2023
	COE 16	1316	2005-2023
	HILLY WASH	407	2007-2023
	INGRAM'S Bay North	385	2008-2009, 2011-2023
	DAYS POINT	40	2003-2023
	POINT OF SHOALS	123	2003-2023
	WRECK SHOAL	174	2003-2023
	CROSS ROCK	198	2003-2023
	MULBERRY POINT	226	2003-2023
	UPPER DEEP WATER SHOAL	326	2003-2023
	LOWER DEEP WATER SHOAL	327	2004, 2006-2023
	UPPER	328	2003-2023
	HORSEHEAD MIDDLE	329	2003-2023
	HORSEHEAD LOWER	330	2003-2023
	HORSEHEAD	331	2003-2023
	MOON ROCK	332	2003-2023
	V-ROCK	332	2003-2023
	SHANTY ROCK	335	2003-2023
	DRY SHOAL	336	2003-2023
	SWASH	338	2003-2023
	UPPER JAIL ISLAND	339	2003-2023
	SWASH MUD SLOUGH	340	2003-2023
	OFFSHORE SWASH	341	2003-2023
	LOWER JAIL ISLAND	342	2003-2008, 2010, 2012, 2014-2023
	OFFSHORE JAIL ISLAND	343	2003-2023
	HOTEL ROCK	346	2003-2005, 2007-2023
	SNYDER'S ROCK	347	2004-2005, 2007-2023

River (<i>R</i>)	Reef Name	Reef ID (<i>r</i>)	Years (<i>t</i>)
Piankatank River	TRIANGLE ROCK	348	2003-2023
	BALLARD'S MARSH	370	2006-2023
	UPPER THOMAS ROCK	373	2007-2008, 2010-2023
	LOWER THOMAS ROCK	374	2006-2023
	UPPER DOG SHOAL	375	2006-2008, 2010-2023
	HIGH SHOAL WHITE SHOAL	377	2006-2023
	UPPER BROWN SHOAL	169	2015-2023
	LOWER BROWN SHOAL	410	2015-2023
	LOWER BROWN SHOAL	411	2015-2023
	BLAND POINT	8	2003, 2006-2023
	BURTON POINT A	20	2003, 2006-2023
	CAPE TOON GINNEY POINT	24	2003, 2006-2023
	GINNEY POINT	50	2003, 2006-2023
	PALACE BAR A	110	2003-2004, 2006-2023
	STOVE POINT	140	2006-2023
	FISHING POINT	395	2010-2023
	LOWER EDGE EAST	1004	2003-2023
	BROAD CREEK	1007	2003-2023
	NORTH END	1010	2003, 2006-2008, 2010-2013, 2015-2023
	DRUMMING GROUND OFFSHORE	1018	2005-2023

**Rappahannock River
(includes the Corrotoman
River)**

River (R)	Reef Name	Reef ID (r)	Years (t)
	DRUMMING GROUND INSHORE	1019	2003-2004, 2006-2023
	BROAD CREEK INSHORE	1028	2003, 2005-2023
	BUTLER'S HOLE WEST	1053	2008-2023
	BROAD CREEK	1061	2007-2023
	SANCTUARY BUTLER'S HOLE	1064	2007-2023
	SANCTUARY BUTLER'S HOLE GRAVEL PLANT	1067	2015-2023
Tangier and Pocomoke Sounds	JOHNSON'S ROCK	1131	2006-2023
York River and Mobjack Bay (includes the East River)	ABERDEEN ROCK	1	2009-2023
	PAGE'S ROCK	109	2009, 2011-2023
	TIMBERNECK	389	2009-2023

After selecting included reefs, there were river-reef-year combinations, denoted by (R, r, t) , that had a sample size that was too small for the fitting software to produce model results. As such, we created “spat condition” and “live condition” labels for each (R, r, t) th sample (**Table 2**): a log-normal distribution was only fit to spat oysters with at least 25 animals; a GMM was only fit to live oysters with at least 50 animals; whenever a distribution was fit, the sample was flagged if there were less than 50 spat or less than 250 live oysters in that sample (Figure 2), suggesting that any software output for flagged samples could be unreliable.

Table 2: Protocol for combinations of spat and live sample sizes for each (R, r, t) th sample. *Note that the numerical computations in `McLust`, `MASS`, and other model-fitting software tend to break down with too few observations.

	$n_{Rrt}^{(spat)} > 50$	$25 < n_{Rrt}^{(spat)} \leq 50$	$n_{Rrt}^{(spat)} < 25^*$
$n_{Rrt}^{(live)} > 250$	<ul style="list-style-type: none"> • Log-normal distribution fit to spat SL data • GMM fit to live SL data 	<ul style="list-style-type: none"> • Log-normal distribution fit to spat SL data, but flagged as a small sample size in data visualizations • GMM fit to live SL data 	<ul style="list-style-type: none"> • No log-normal (spat data pre-emptively excluded to prevent software breakdown) • GMM fit to live SL data
$50 < n_{Rrt}^{(live)} \leq 250$	<ul style="list-style-type: none"> • Log-normal distribution fit to spat SL data • GMM fit to live SL data, but flagged as a small sample size in data visualizations 	<ul style="list-style-type: none"> • Log-normal distribution fit to spat SL data, but flagged as a small sample size in data visualizations • GMM fit to live SL data, but flagged as a small sample size in data visualizations 	<ul style="list-style-type: none"> • No log-normal (spat data pre-emptively excluded to prevent software breakdown) • GMM fit to live SL data, but flagged as a small sample size in data visualizations
$n_{Rrt}^{(live)} < 50^*$	<ul style="list-style-type: none"> • Log-normal distribution fit to spat SL data • No GMM, too small to reliably estimate any clusters 	<ul style="list-style-type: none"> • Log-normal distribution fit to spat SL data, but flagged as a small sample size in data visualizations • No GMM, too small to reliably estimate any clusters 	<ul style="list-style-type: none"> • No log-normal (spat data pre-emptively excluded to prevent software breakdown) • No GMM, too small to reliably estimate any clusters

Given the necessarily right skewed distribution for spat SL (Figure 2a) and

often multimodal distribution for live oyster SL (Figure 2b), we fit a log-normal distribution to spat SL data from each (R, r, t) th sample and a GMM to live oyster SL data from that same (R, r, t) th sample.

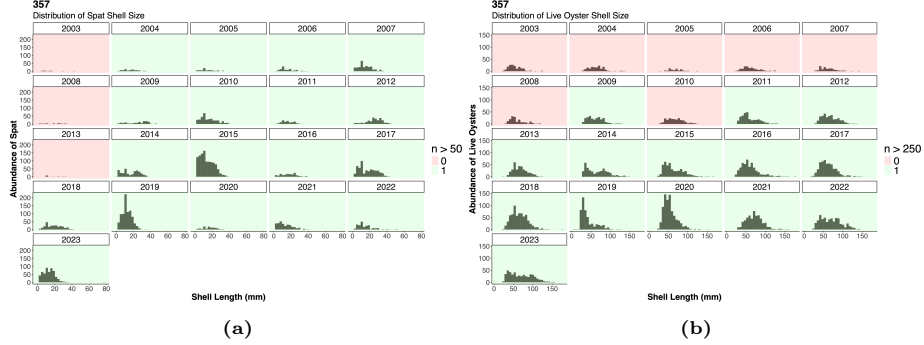


Figure 2: Annual empirical distributions of shell length in reef 357 for spat (a) and live oysters (b).

3 Methodology

3.1 Overview

We fit a log-normal distribution to the spat SL data to estimate the mean, $\mu_{Rrt}^{(0)}$, and standard deviation, $\sigma_{Rrt}^{(0)}$ (see Section 3.2).

To estimate Gaussian components of live oysters using the distribution of SL data, we fit initial GMMs based on how reef-level features compared to stratum-level features of these data. Let the estimated mean and standard deviation of SL for the k th Gaussian component of live oysters be $\hat{\mu}_{Rrt}^{(k)}$ and $\hat{\sigma}_{Rrt}^{(k)}$, respectively. By comparing $\hat{\mu}_{Rrt}^{(k)}$ to the 80th percentile of the (R, t) th distribution of SL (combining all reefs in the same river stratum), we assigned an age $\hat{a}_{Rrt}^{(k)}$ (ranging from two to five) to this component and updated the initial estimates $\hat{\mu}_{Rrt}^{(k)}$ and $\hat{\sigma}_{Rrt}^{(k)}$, if necessary (see Section 3.3). Then, we developed an algorithm to link the spat and live components¹ over time t to identify cohorts (see Section 3.4).

Specifically, let Y_{Rrti} be the SL of the i th observed oyster (spat or live) from the (R, r, t) th sample. Denote the unknown population proportions of spat and live age classes by

$$\pi_{Rrt}^{(k)} \quad \text{for } k = k_{Rrt} = 0, 1, 2, \dots, G_{Rrt}$$

where $k = 0$ denotes spat oysters, $k > 0$ denotes the k th age class of live oysters,

¹The term ‘‘component’’ is used loosely in reference to spat data.

and G_{Rrt} is the unknown number of live age classes. Then, our initial reef-level model for SL was

$$Y_{Rrti} \sim \begin{cases} \text{log-normal with } E(Y_{Rrti}) = \mu_{Rrt}^{(0)} \text{ and } SD(Y_{Rrti}) = \sigma_{Rrt}^{(0)} & \text{if } i\text{th oyster was spat,} \\ \mathcal{N}(\mu_{Rrt}^{(k)}, \sigma_{Rrt}^{(k)}) & \text{if } i\text{th oyster was live} \end{cases}$$

and

$$P(Y_{Rrti}^{(live)} \text{ is from the } k\text{th age class}) = \pi_{Rrt}^{(k)}, \quad \sum_{k=1}^{G_{Rrt}} \pi_{Rrt}^{(k)} = 1 - \pi_{Rrt}^{(0)}$$

Thus, we assumed that each k th Gaussian component of SLs represents an age class with $a_{Rrt}^{(k)}$ years of age (unknown except $a_{Rrt}^{(0)} \equiv 1$ for spat). Age estimation involved river-level GMM alongside the above reef-level GMM, allowing river-level features of SL to deviate from stratum-specific structure on initial reef-level GMM estimates. Below are details for the derivation of G_{Rrt} , parameter estimates $\{\hat{\mu}_{Rrt}^{(k)}, \hat{\sigma}_{Rrt}^{(k)}, \hat{\pi}_{Rrt}^{(k)}, \hat{a}_{Rrt}^{(k)}\}$, and our cohort identification algorithm.

3.2 Details of spat oyster analysis

First, we assigned $\hat{\pi}_{Rrt}^{(0)}$ to equal the proportion of spat relative to live oysters in each (R, r, t) th sample, such that

$$\hat{\pi}_{Rrt}^{(0)} = \frac{n_{Rrt}^{(spat)}}{n_{Rrt}^{(spat)} + n_{Rrt}^{(live)}}$$

Next, we used the `MASS:fitdistr` function to determine $\hat{\mu}_{Rrt}^{(0)}$ and $\hat{\sigma}_{Rrt}^{(0)}$ for spat SL. Finally, we assigned $\hat{a}_{Rrt}^{(0)} = 1$ due to the knowledge that spat are the youngest oysters of the year.

3.3 Details of Gaussian Mixture Modeling to live oyster SL data

3.3.1 Model parameters

A mixture distribution is a probability distribution obtained as a convex linear combination of probability density functions (Scrucca et al., 2023). The individual distributions for the (R, r, t) th sample are mixture components labeled k_{Rrt} , and the weights associated with all G_{Rrt} components are mixture probabilities $\tilde{\pi}_{Rrt}^{(k)}$ ($\tilde{\pi}_{Rrt}^{(k)} > 0$ and $\sum_{k=1}^{G_{Rrt}} \tilde{\pi}_{Rrt}^{(k)} = 1$) for $k = k_{Rrt} = 1, 2, \dots, G_{Rrt}$. We fit the following univariate finite Gaussian mixture distribution

$$\sum_{k=1}^{G_{Rrt}} \tilde{\pi}_{Rrt}^{(k)} f_{Rrt}^{(k)}(Y_{Rrt}; \mu_{Rrt}^{(k)}, \sigma_{Rrt}^{(k)})$$

where $f_{Rrt}^{(k)}(\cdot)$ is the density of the k th Gaussian component of the (R, r, t) th sample and Y_{Rrt} is the vector of shell lengths of live oysters.

We fit this model, with no specified covariance structure, using the `mclust` package (Scrucca et al., 2023). We allow the `mclust::Mclust` function to decide the value for G_{Rrt} from 1 to 4, reflecting our current understanding that four-year-old oysters (in their 5th year) are rare in Chesapeake Bay (Harding et al., 2010; Southworth et al., 2010). The `Mclust` function uses an expectation-maximization algorithm and the Bayesian information criterion (BIC) to select the best model and best fit of G_{Rrt} . Scrucca et al. (2023) and Neath & Cavanaugh (2012) recommend that $\Delta_{BIC} \gtrsim 6$ suggests strong evidence in favor of one model over the other. The `mclust::Mclust` function automatically selects the best fitting model (largest BIC), regardless of the amount of evidence in favor of the “best model”. As such, we manually selected the more parsimonious model when there was weak evidence in favor of one model over the other ($\Delta_{BIC} < 2$).

We posit that each component k_{Rrt} should have varying variances (represented by a “V” model), as opposed to an “E” model with equal variances (see documentation in Scrucca et al. (2023)) unless there is strong evidence against it. As such, for each (R, r, t) th GMM where $\Delta_{BIC} < 2$, we extracted the BIC of all models ($1 \leq G_{Rrt} \leq 4$) of varying variance “V”. We calculated Δ_{BIC} between all model fits with varying variance “V” and the “best-fitting” model determined by `mclust::Mclust`. For the “V” models whose $\Delta_{BIC} < 2$ when compared to the “best-fitting” model, we selected the “V” model with the smallest G_{Rrt} . If there was no “V” model that met these criteria, we repeated the process to pick the most parsimonious “E” model.

The `Mclust` function sets $\sum_{k=1}^{G_{Rrt}} \tilde{\pi}_{Rrt}^{(k)} = 1$. Since each (R, r, t) th sample includes spat ($k = 0$) and live components ($k = k_{Rrt} = 1, 2, \dots, G_{Rrt}$), we adjusted $\tilde{\pi}_{Rrt}^{(k)}$ by taking

$$\hat{\pi}_{Rrt}^{(k)} = \tilde{\pi}_{Rrt}^{(k)} (1 - \hat{\pi}_{Rrt}^{(0)})$$

so that

$$\sum_{k=1}^{G_{Rrt}} \hat{\pi}_{Rrt}^{(k)} = (1 - \hat{\pi}_{Rrt}^{(0)}) = \frac{n_{Rrt}^{(live)}}{n_{Rrt}^{(spat)} + n_{Rrt}^{(live)}}$$

The adjusted mixture weights $\hat{\pi}_{Rrt}^{(k)}$'s were then used for cohort identification in Section 3.4.

3.3.2 Age estimation and updates to reef-level estimates

Given that the shape and size of oysters tend to vary based on environment (typically at a stratum-level as opposed to a reef-level (Marquardt et al., 2024)), each k_{Rrt} th (reef-level) Gaussian component was estimated to have age $\hat{a}_{Rrt}^{(k)}$ based on its comparison to river-level data, as follows. First we combined spat and live oysters sampled from the same (R, t) th combination (fixed river stratum, fixed year) *i.e.*, $Y_{Rt} = \{Y_{Rrti} : \text{all } i \text{ and all } r \text{ from } R \text{ even if } r \text{ was excluded from reef-level analyses}\}$. We used `Mclust` to fit the river-level Gaussian mixture model

$$\sum_{m=1}^{G_{Rt}} \pi_{Rt}^{(m)} f_{Rt}^{(m)}(Y_{Rt}; \mu_{Rt}^{(m)}, \sigma_{Rt}^{(m)})$$

where G_{Rt} is the number of mixture components ($1 \leq G_{Rt} \leq 4$), $f_{Rt}^{(m)}(\cdot)$ is the density of the m th Gaussian component of the (R, t) th river stratum (with $m = 1, \dots, G_{Rt}$), the $\pi_{Rt}^{(m)}$'s are the mixture weights ($\pi_{Rt}^{(m)} > 0$ and $\sum_{m=1}^{G_{Rt}} \pi_{Rt}^{(m)} = 1$), and $\mu_{Rt}^{(m)}$ and $\sigma_{Rt}^{(m)}$ are the Gaussian parameters of the m th density component. Similarly to the GMMs at the (R, r, t) th level, we manually selected the more parsimonious model when there was weak evidence of difference between models ($\Delta_{BIC} < 2$).

This Gaussian mixture model at the (R, t) th level allows us to employ our understanding of the age structure at each R th river stratum. We determined that the 80th quantile was an appropriate cutoff for estimating ages², the youngest age set to 2 (*i.e.*, a year older than spat). The estimation mechanism is as follows:

- $q_{Rt}^{(0)} = 0$
- Fix R, r , and m . Determine $q_{Rt}^{(m)} = 80\text{th percentile of } \mathcal{N}(\hat{\mu}_{Rt}^{(m)}, \hat{\sigma}_{Rt}^{(m)})$ for $m > 0$
- For each $k_{Rrt} = 1, \dots, G_{Rrt}$: if $q_{Rt}^{(m-1)} < \hat{\mu}_{Rrt}^{(k)} \leq q_{Rt}^{(m)}$ then $\hat{a}_{Rrt}^{(k)} := m + 1$
- Repeat over all (R, t, m) .

When $G_{Rt} = 1$, $\hat{a}_{Rrt}^{(k)}$ is assigned ‘‘N.A.’’, meaning that there was no useable knowledge about the size of live age groups (age 2+) in that river system, and as such, we could not reasonably assign $\hat{a}_{Rrt}^{(k)}$.

²Preliminary sensitivity analyses (not shown) suggested robustness of our method to the choice of this cutoff.

Next, initial reef-level $\hat{\mu}_{Rrt}^{(k)}$ and $\hat{\sigma}_{Rrt}^{(k)}$ from Section 3.3.1 were subject to updating based on GMM fits to reef-level data, whenever $\hat{a}_{Rrt}^{(k)} = \hat{a}_{Rrt}^{(k')}$ for $k \neq k'$. The reason is as follows.

In an (R, r, t) th population, the true age $a_{Rrt}^{(k)}$ cannot be identical for different values of k if age dictates SL (*i.e.*, at the same reef in the same year, two separate Gaussian components cannot have the same age). Although recruitment could have continued after each sampling date, by the time sampling occurs the following fall, all spat oysters from the previous sample tend to be aggregated into similar sizes identifiable as live oysters. Therefore, we ignored possible new recruits among live oysters and calculated the following updated estimates to pool those components sharing the same age assignment into one:

$$\hat{\mu}_{pooled} = \sum_{k=1}^{p_{Rrt}} \hat{\pi}_{Rrt}^{(k)} * \hat{\mu}_{Rrt}^{(k)}$$

$$\hat{\sigma}_{pooled}^2 = \left[\sum_{k=1}^{p_{Rrt}} \hat{\pi}_{Rrt}^{(k)} (\hat{\sigma}_{Rrt}^{2(k)} + \hat{\mu}_{Rrt}^{2(k)}) \right] - \hat{\mu}_{pooled}^2$$

where p_{Rrt} is the number of components in the same (R, r, t) th sample showing the same value for $\hat{a}_{Rrt}^{(k)}$. In these instances, $\hat{\mu}_{pooled}$ and $\hat{\sigma}_{pooled}$ were used in the cohort assignment algorithm.

3.4 Cohort assignment algorithm

The following algorithm was used to link spat and live components over time to form age cohorts ($\hat{c}_{Rrt}^{(k)}$).

Algorithm 1: Cohort Assignment Algorithm for determination of cohort label $\hat{c}_{Rrt}^{(k)}$ ³

Input: Dataframe \mathbb{D} with column headings $\{R, r, t, k, \hat{\mu}_{Rrt}^{(k)}, \hat{a}_{Rrt}^{(k)}, \hat{c}_{Rrt}^{(k)}\}$ collating all component means and their estimated ages after any necessary pooling.
// All values of $\hat{c}_{Rrt}^{(k)}$ initiated as "N.A."

1. **Assign** column $\hat{c}_{Rrt}^{(k)} := "t.\hat{a}_{Rrt}^{(k)}"$ // Unique unless $\hat{a}_{Rrt}^{(k)} := "N.A."$
2. **for** $R = 1, 2, \dots, 7$ **do** // River stratum label
3. **for** $r = 1, 2, \dots, n_R$ **do** // reef label, n_R in total

³Note that our implementation of this algorithm employed a different set of labels.

```

4.   for  $t = 2003, 2004, \dots, 2022$  do

      4.1. Extract from  $\mathbb{D}$  the  $(R, r, t)$ th dataframe  $\mathbb{D}_{Rrt}$  with column headings
       $\{R, r, t, k, \hat{\mu}_{Rrt}^{(k)}, \hat{a}_{Rrt}^{(k)}, \hat{c}_{Rrt}^{(k)}\}$ 

      4.2. Extract from  $\mathbb{D}$  the  $(R, r, t + 1)$ th dataframe  $\mathbb{D}_{R,r,t+1}$  with column
      headings  $\{R, r, t + 1, k', \hat{\mu}_{R,r,t+1}^{(k')}, \hat{a}_{R,r,t+1}^{(k')}, \hat{c}_{Rrt}^{(k')}\}$ 

5.   for each  $k$ th row in  $\mathbb{D}_{Rrt}$  do

      5.1. Extract  $(k')$ th row from  $\mathbb{D}_{R,r,t+1}$  for which  $\hat{a}_{R,r,t+1}^{(k')} == \hat{a}_{R,r,t}^{(k)} + 1$ 
      // can be  $\emptyset$ 

      5.2. if 5.1 is not  $\emptyset$  then

          5.2.1. if  $\hat{\mu}_{R,r,t+1}^{(k')} > \hat{\mu}_{R,r,t}^{(k)}$  then update  $\hat{c}_{R,r,t+1}^{(k')} := \hat{c}_{R,r,t}^{(k)}$ 
          // same cohort

6.   end loop  $t$     //  $\mathbb{D}$  is now updated with new  $\mathbb{D}_{R,r,t+1}$ 

7.   end loop  $r$ 

8. end loop  $R$ 

```

After running the algorithm, any components labeled "N.A." in column $\hat{c}_{Rrt}^{(k)}$, were given unique labels ("N.A.1", "N.A.2" , ... , $n_{N.A.}$) where $n_{N.A.}$ is the number of components assigned "N.A." in each (R, r, t) th sample.

4 Algorithm output

First, we discuss the algorithm output for two reefs, namely reef 357 in the Chesapeake Bay Mainstem (Figure 3) and reef 331 in the James River (Figure 4). The discussion illustrates the utility of our approach.

For the first few years of sampling ($t = 2003-2008, 2010$), reef 357 had an insufficient amount of data (pink years and/or asterisks in Figure 3) and therefore a small number of age groups, many of which could not be linked. During this time frame, recruitment (shown by age one, *i.e.*, spat groups) was consistent, suggesting that spat formed the dominant age group during those years. As time progressed, live oysters were more abundant on the reef, spat (and therefore recruitment) continued to be consistent, and cohort lifespan began to lengthen, shown by the presence of older age groups. This same trend was found in reef 312, the other reef analyzed in the Chesapeake Bay Mainstem, though reef 312 had more years with insufficient amounts of data. In reef 357, there were two cohorts whose terminal age was five, compared to one in reef 312, as

of 2023. Most oysters were smaller than the market size in Virginia (generally set at 76 mm throughout this time period), shown by the few error bars above the orange dotted line. In the latter decade, cohorts could be tracked for longer periods and were living longer (Figure 3). In the last few years, oysters may or may not grow to four or five years old, because we do not have the data after 2023 to estimate their lifespan. The mean shell size of spat oysters were relatively stable across the entire time period.

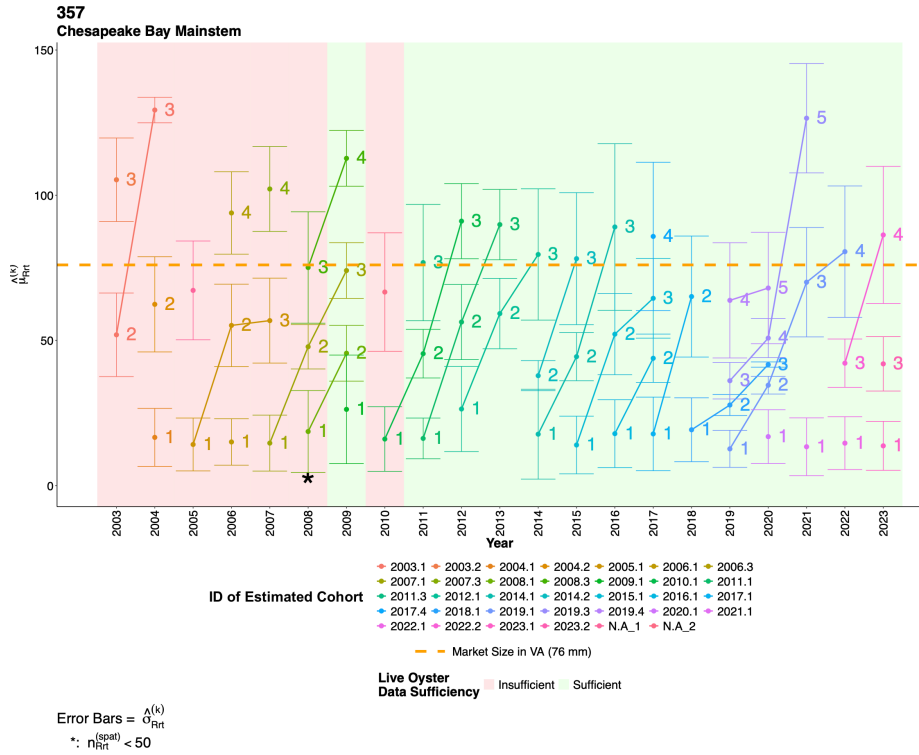


Figure 3: Temporal visualization of estimated cohorts $\hat{c}_{Rrt}^{(k)}$ in Reef 357 in the Chesapeake Bay Mainstem. Points represent $\hat{\mu}_{Rrt}^{(k)}$ and error bars represent $\hat{\sigma}_{Rrt}^{(k)}$ of the estimated components. A green panel background represents $n_{Rrt}^{(live)} > 250$, while a pink panel background represents $n_{Rrt}^{(live)} \leq 250$. A black asterisk (*) represents $n_{Rrt}^{(spat)} < 50$. The number next to each point represents $\hat{a}_{Rrt}^{(k)}$. The orange dotted line represents the market size in Virginia (76 mm). The figures for all the reefs analyzed can be found in Appendix X.

Reef 331 in the James River (Figure 4) was sampled consistently throughout the entire time frame, though from 2003 to 2005, recruitment was poor, as suggested by the lack of reliable log-normal parameter estimates due to insufficient spat data. Older age cohorts were found throughout the time series as well. Many of the age groups could be linked together, suggesting longevity of cohorts. All error bars after 2010 were below market size in Virginia. This

pattern is common in all reefs ($n_R = 31$) in the James River (Appendix).

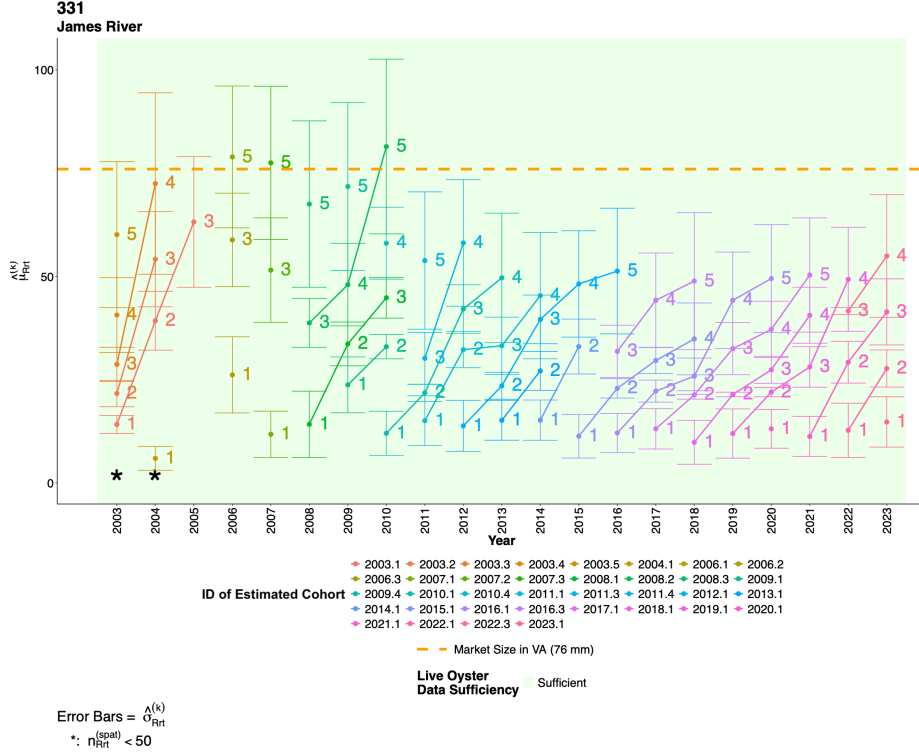


Figure 4: Temporal visualization of each algorithm output for Reef 331 in the James River.

The patterns shown in reef 357 and reef 331 support the findings of differences in size and growth of oysters in different river systems by Marquardt et al. (2024). In general, oysters in the James River are smaller than oysters in the Chesapeake Bay Mainstem, but both exhibit signals of reduced age-truncation despite signals of shell shrinkage. Oysters in the James River more consistently lived to an estimated four and five years old compared to other tributaries in Virginia’s Chesapeake Bay. The lines connecting components into estimated cohorts tend to be longer and less steep for reef 331 then for reef 357, indicating longer-lived, but slower-growing cohorts for this and other reefs in the James (given the similar patterns across the James reefs we analyzed).

The above results for these reefs suggest that cohorts could be reasonably estimated using our method. When the year-specific distributions for each cohort in reef 357 (Chesapeake Bay Mainstem) are combined in a single display (as a pane in Figure 5), distributions rarely overlap much, allowing a clear temporal tracking of growth in size, while relative abundance $\hat{\pi}_{Rrt}^{(k)}$ decreased, possibly due to oysters dying off as they aged. The distributions of all cohorts identified

for all 64 reefs can be found in the Appendix.

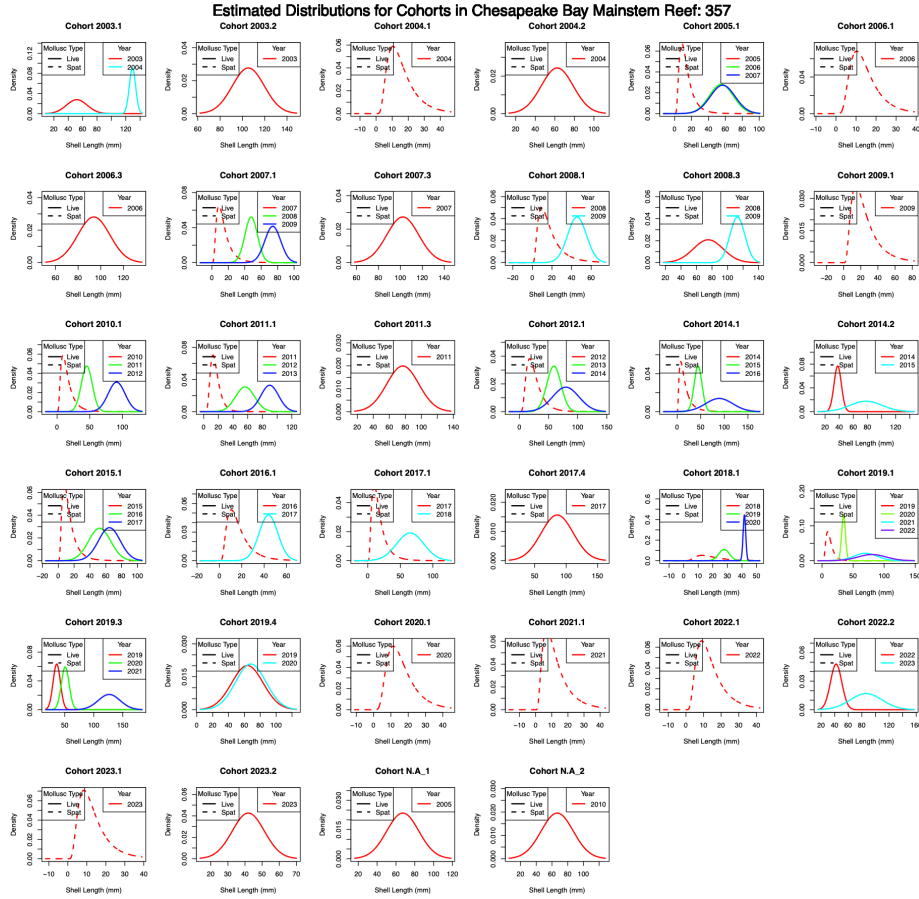


Figure 5: Estimated distributions for cohorts in Chesapeake Bay Mainstem reef 357. Each pane refers to a different identified cohort ($\hat{c}_{Rrt}^{(k)}$). Note that the mixture weights of each cohort ($\hat{\pi}_{Rrt}^{(k)}$) do not sum to one because each component k is linked over time, while the GMM (with its mixture weights) was estimated yearly.

5 Signals of resiliency

5.1 Age-truncation

For almost all reefs in our analysis, older age groups (*i.e.*, $\hat{a}_{Rrt}^{(k)} \geq 4$) were more present in the second decade of the time series, suggesting that age-truncation issues was improving in Virginia’s Chesapeake Bay. In the Chesapeake Bay Mainstem (Figure 6a), older age groups were present more frequently in the latter decade (2014-2023) compared to the first decade. For reef 312, a

four-year-old age group was not estimated until 2019, then found almost every year after. Further, in any latter year, the age structure was more diverse, meaning that there were more age groups living on a reef at the same time. This trend was seen in all of Virginia’s tributaries, except in the James River (see Appendix). In the James River (Figure 6b), older age groups were consistently present across the time series, and a multi-year-class age structure was much more common.

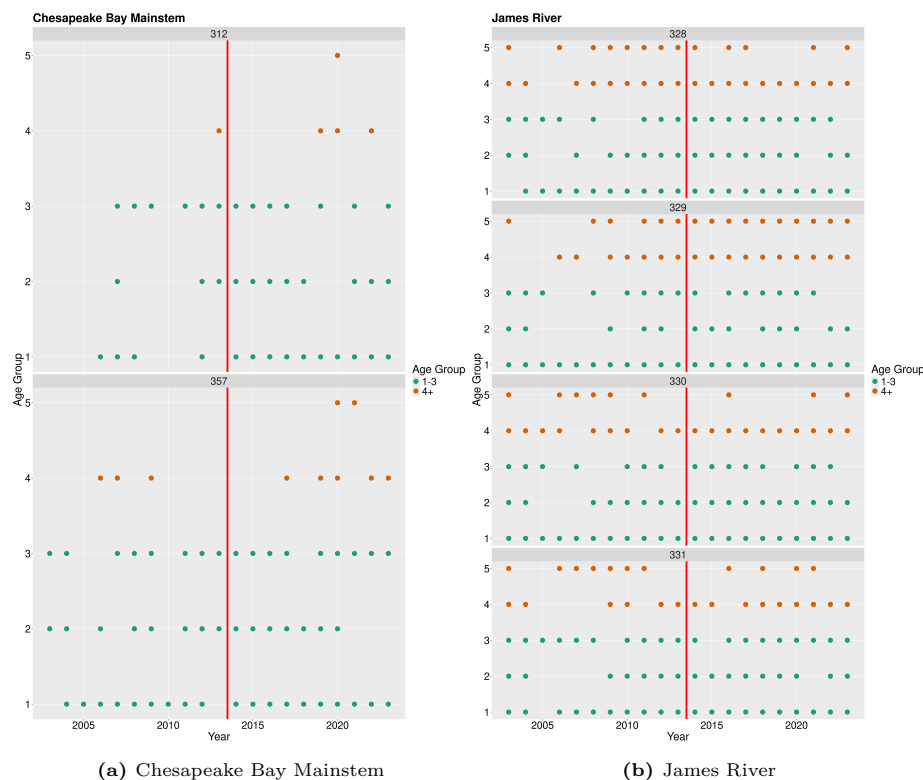


Figure 6: Age structure over time in each analyzed reef from the Chesapeake Bay Mainstem (a) and select analyzed reefs from the James River (b). The red line represents the midpoint in the 21-year time series (2013). Green dots represent estimated ages of one to three and orange dots four and older.

5.2 Shell size shrinkage

When comparing the distribution of SL of estimated age groups ($\hat{a}_{Rrt}^{(k)}$) between decades, we found evidence of shell size shrinkage over time. Within the same estimated age group, estimated distributions of SL were made up of larger values in the first decade compared to the second, shown in green and brown, respectively, in Figure 7. This trend was found in all analyzed reefs, but strongest in Chesapeake Bay Mainstem (Figure 7a) and James river reefs

(Figure 7b). For both river systems, this trend was less apparent for spat (*i.e.*, $\hat{a}_{Rrt}^{(k)} = 1$).

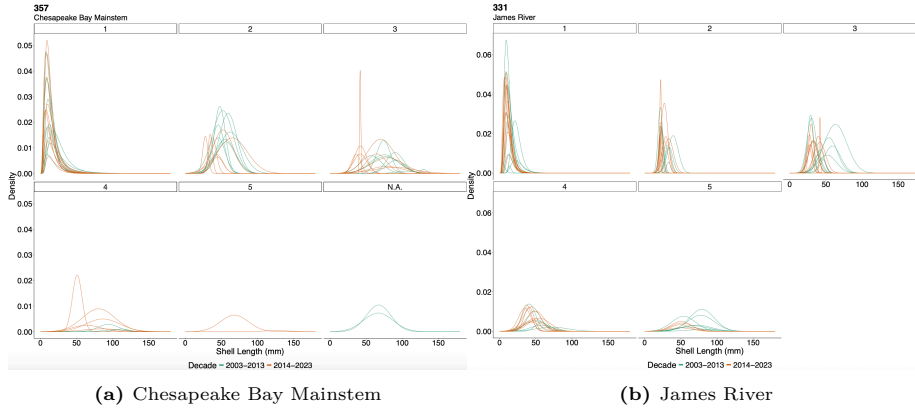


Figure 7: SL distributions of each estimated age group, colored by decade, for Chesapeake Bay Mainstem reefs (a) and selected reefs in the James River (b). The facet labels represent each $\hat{a}_{Rrt}^{(k)}$. Figures for all 64 reefs can be found in the Appendix.

6 Discussion

6.1 Method utility

This research demonstrates a practical method for identifying age groups and linking them into cohorts solely based on SL data observed across space and time. This method allows one to conduct an age-structure analysis at the most spatially granular level (oyster reefs, r), while incorporating information about the corresponding river system or tributary (R), facilitating the comparison of the age structure and oyster shell size across river systems. Though consistent sampling for consecutive years (here, we considered at least eight consecutive years) is required, this method could be applied to other managed species that do not have adequate age data, and age-structured management approaches are desired. Future studies could apply this method to analyze growth, mortality, and shell accretion rates similar to previous studies in Chesapeake Bay (Harding et al., 2010; Mann et al., 2009; Marquardt et al., 2024; Southworth et al., 2010). Though practical for estimating and identifying age groups based on SL data only, the method has limitations. In a few instances, a live age group ($\hat{a} \geq 2$) would not be linked to any spat group ($\hat{a} = 1$), which is biologically illogical.

For our complex objective of gaining bay-level insights informed by river- and reef-level understanding—all based on animal-level data—a fully rigorous methodology may be a Bayesian hierarchical model (BHM) that captures bay-wide features through bay-level model parameters, with river-specific age-class structure informed by bay-level parameters, and reef-specific age-class structure

informed by river-level structure. However, developing a viable initial model for such a complex model hierarchy requires and in-depth exploratory data analysis (EDA). The method in this paper is a tool that facilitates comprehensive data visualizations for this objective. For example, a BHM framework for these data would require a type of mixed membership model (*e.g.*, see Erosheva & Fienberg (2005)) that either (a) regards each G_{Rrt} and G_{Rt} as an unknown parameter, or (b) relies on fitting the full model hierarchy for different combinations of G_{Rrt} and G_{Rt} . The implementation of option (a) is typically very complex and computationally intensive, unless G_{Rrt} and G_{Rt} are constrained by highly informative priors (*e.g.*, see Stephens (2000)) that may result in unwanted bias. Option (b) requires the enumeration of all plausible combinations of G_{Rrt} and G_{Rt} , and the comparison of model performance among the entire set of corresponding BHM fits, so that the best performing set of G_{Rrt} and G_{Rt} values can be identified. In other words, neither (a) nor (b) is practical without some guidance based on an in-depth EDA. Our method can be regarded as the EDA counterpart of option (b), thus, not only does it reduce the computational burden that is required to fit a very large number of complex BHMs, but it also provides data visualizations that shed light on the ecological phenomena of age-class structure, lifespan, and resilience, all in a holistic manner.

6.2 Implications for resiliency

Our research suggests that older age classes are becoming more common throughout Virginia’s Chesapeake Bay. Compared to studies in the 2010s (Harding et al., 2010; Mann et al., 2009; Southworth et al., 2010), we found that age three-and-older oysters have been present more frequently, especially in the second decade (2014-2023). Between 1998 and 2009, nearly no oysters of age four were identified by Harding et al. (2010). Our study identified that age four-and-older oysters were present very consistently after 2013. Before 2009, year-one and year-two age classes in the James River had very high mortality rates despite consistently strong recruitment (Mann et al., 2009). Our study found consistent age groups from one to five, although they were more similar in size (mostly less than market size of 76 mm). This suggests that our more rigorous method may be better equipped to identify age groups in systems under stress compared to previous methods applied (*e.g.*, Bhattacharya, 1967; Mildemberger et al., 2017). Further, previous studies in Chesapeake Bay aggregated oysters into 2-mm bin sizes (Harding et al., 2010; Mann et al., 2009; Southworth et al., 2010), which may have masked the small size differences between ages two through four. We identified some age-six classes in reefs in the James and Piankatank Rivers (see Appendix), suggesting that in terms of age structure, the oyster reef population in Chesapeake Bay could be improving due to resiliency, especially to disease. This is because the epizootics of *Perkinsus marinus* and MSX lead to high mortality events, particularly of larger (older) oysters, controlled by salinity and temperature (Andrews, 1988; Kusnerik et al., 2018). Thus, the presence of older age groups suggests greater survival than previously estimated by Harding et al. (2010), Mann et al. (2009); and Southworth et al. (2010).

Our research found additional evidence of resiliency, through the continuation of shell size shrinkage over time while remaining alive. Many cohorts are less than market size in Virginia (76 mm), a similar finding to previous studies (Mann et al., 2022). This “shrinking” trend is most apparent in the James River, which historically has the largest acreage of productive bottom and highest average annual production (Haven & Whitcomb, 1986). The shrinking trend is least pronounced in the Piankatank and Great Wicomico rivers, two river systems that have received shell plantings since the 1960s, and designated sanctuary reefs through modern large-scale restoration efforts (Schulte, 2017). Nonetheless, oysters larger than 51 mm are very susceptible to mortality from *MSX*, which could explain smaller shell sizes throughout the region in recent years (Kusnerik et al., 2018). Further, adult oysters display decreased growth rates and calcification rates in response to ocean acidification (Lemasson et al., 2017). These factors and their interactions with salinity and temperature could be contributing to the signal of increased lifespan, despite environmental decline.

There are two main hypotheses for explaining shell size shrinkage over time. The first suggests human-induced shrinking: fisheries science research has suggested that harvesting pressure on bigger, faster growing animals has selected for slow-growing, smaller, animals over time (Allendorf & Hard, 2009; Rutter, 1902). The second suggests environmental-induced shrinking, such as disease prevalence and coastal acidification could be drivers that slow the growth and terminal size of oysters (Kusnerik et al., 2018; Lemasson et al., 2017; Ross et al., 2024; Rybovich et al., 2016). In particular, coastal and ocean acidification has the potential to be an increasingly important contributor to oyster challenges in Chesapeake Bay (Boulais et al., 2017; Lemasson et al., 2017; Waldbusser et al., 2011). These hypotheses have yet to be explored directly and holistically in relation to resiliency for eastern oysters in the Chesapeake Bay.

Our results suggest that eastern oysters are displaying enhanced resiliency, due to increased longevity of cohorts, despite continued environmental decline, exhibited by shell size shrinkage over time. These smaller (yet older) age groups contribute less shell to the reef, suggesting a complex push-and-pull in terms of self-sustainability in the future. The current framework of ecological resiliency does not aid resource management in these complex situations. Standard ecological definitions of “resiliency”, an inherently abstract concept, are difficult to define. Baskett et al. (2014) defines “resiliency” as the probability of maintaining a given state (ecological resilience) and the rate of return to a given state following a disturbance (engineering resilience). National Academies of Science, Engineering, and Medicine (2019) defines resiliency the ability to survive despite climate change. These definitions lack an explicit description of the metrics that should be measured and the spatiotemporal scale at which to do so. Our goal is to address the knowledge gap as we progress in our research.

7 Conclusion

Our paper is the first study on Virginia’s Chesapeake Bay oysters that estimates age groups and link them into age cohorts over an expansive spatiotemporal scale. This method facilitated the identification, tracking, and aging of oyster cohorts, and subsequently revealing signals of resiliency. The results suggest that in the post-epizootic period (post 2005) and period where ecosystem management is stable (post 2009), age-truncation is being reversed, despite continued shell size shrinkage in recent years. Mann & Powell (2007) call for novel and alternative approaches that address oyster restoration holistically, and our method provides an avenue to rigorously guide the formal modeling of age structure and the identification of river systems that have not rebuilt and may require a shift in management strategy. Our results suggest that this type of modeling has the potential to reveal that differences in management strategies, despite continued environmental decline, could be contributing to resiliency in Virginia’s Chesapeake Bay oyster reefs.

8 Acknowledgements

This research was supported by award #24970 from the Chesapeake Bay Trust-Chesapeake Oyster Alliance Chesapeake Oyster Innovation Award. The authors acknowledge William & Mary Research Computing for providing computational resources and/or technical support that have contributed to the results reported within this paper (<https://www.wm.edu/offices/it/services/researchcomputing/atwm/>)

9 Data availability statement

The data, code, and interactive maps of the results are available at the following GitHub repository: <https://go.wm.edu/GsmMyG>.

10 APPENDIX: results for remaining R strata

See results for remaining R strata at the following GitHub repository: <https://go.wm.edu/GsmMyG>

References

Allendorf, F. W., & Hard, J. J. (2009). Human-induced evolution caused by unnatural selection through harvest of wild animals. *Proceedings of the National Academy of Sciences*, 106(supplement_1), 9987–9994. <https://doi.org/10.1073/pnas.0901069106>

- Andrews, J. D. (1988). Epizootiology of the disease caused by the oyster pathogen *Perkinsus marinus* and its effects on the oyster industry. *American Fisheries Society Special Publication*, 18, 47–63.
- Baird, D., & Ulanowicz, R. E. (1989). The seasonal dynamics of the Chesapeake Bay ecosystem. *Ecological Monographs*, 59(4), 329–364. <https://www.jstor.org/stable/1943071>
- Baskett, M. L., Fabina, N. S., & Gross, K. (2014). Response Diversity Can Increase Ecological Resilience to Disturbance in Coral Reefs. *The American Naturalist*, 184(2), E16–E31. <https://doi.org/10.1086/676643>
- Baylor, J. (1895). Survey of oyster grounds in Virginia - report of J.B. Baylor to the governor of Virginia. *Miscellaneous*.
- Bhattacharya, C. G. (1967). A simple method of resolution of a distribution into Gaussian components. *Biometrics*, 23(1), 115. <https://doi.org/10.2307/2528285>
- Bonar, D. B., Coon, S. L., Walch, M., Weiner, R. M., & Fitt, W. (1990). Control of Oyster Settlement and Metamorphosis by Endogenous and Exogenous Chemical Cues. *Bulletin of Marine Science*, 46(2), 484–498.
- Boulais, M., Chenevert, K. J., Demey, A. T., Darrow, E. S., Robison, M. R., Roberts, J. P., & Volety, A. (2017). Oyster reproduction is compromised by acidification experienced seasonally in coastal regions. *Scientific Reports*, 7(1), 13276. <https://doi.org/10.1038/s41598-017-13480-3>
- Coen, L., Luckenbach, M., & Breitburg, D. (1999). The Role of Oyster Reefs as Essential Fish Habitat: A Review of Current Knowledge and Some New Perspectives. *American Fisheries Society Symposium*, 22, 438–454.
- Commission of Fisheries of Virginia. (1954). *Fifty-fourth and fifty-fifth annual reports of the Commission of Fisheries of Virginia (1954)* (p. 63).
- Erosheva, E. A., & Fienberg, S. E. (2005). Bayesian mixed membership models for soft clustering and classification. In C. Weihs & W. Gaul (Eds.), *Classification — the Ubiquitous Challenge* (pp. 11–26). Springer. https://doi.org/10.1007/3-540-28084-7_2
- Fabri-Ruiz, S., Danis, B., Navarro, N., Koubbi, P., Laffont, R., & Saucède, T. (2020). *Benthic ecoregionalization based on echinoid fauna of the Southern Ocean supports current proposals of Antarctic Marine Protected Areas under IPCC scenarios of climate change*. <https://doi.org/10.1111/gcb.14988>
- Grabowski, J. H., Brumbaugh, R. D., Conrad, R. F., Keeler, A. G., Opaluch, J. J., Peterson, C. H., Piehler, M. F., Powers, S. P., & Smyth, A. R. (2012). Economic Valuation of Ecosystem Services Provided by Oyster Reefs. *BioScience*, 62(10), 900–909. <https://doi.org/10.1525/bio.2012.62.10.10>
- Haas, L. W. (1977). The effect of the spring-neap tidal cycle on the vertical salinity structure of the James, York and Rappahannock rivers, Virginia, U.S.A. *Estuarine and Coastal Marine Science*, 5(4), 485–496. [https://doi.org/10.1016/0302-3524\(77\)90096-2](https://doi.org/10.1016/0302-3524(77)90096-2)
- Harding, J. M., Mann, R., Southworth, M. J., & Wesson, J. A. (2010). Management of the Piankatank river, Virginia, in support of oyster (*Crassostrea Virginia*, Gmelin 1791) fishery repletion. *Journal of Shellfish Research*, 29(4), 867–888. <https://doi.org/10.2983/035.029.0421>

- Haven, D. S., & Whitcomb, J. P. (1986). *The public oyster bottoms in Virginia: An overview of their size, location, and productivity*.
- Hemeon, K. M., Ashton-Alcox, K. A., Powell, E. N., Pace, S. M., Poussard, L. M., Solinger, L. K., & Soniat, T. M. (2020). Novel shell stock–recruitment models for *Crassostrea Virginica* as a function of regional shell effective surface area, a missing link for sustainable management. *Journal of Shellfish Research*, 39(3). <https://doi.org/10.2983/035.039.0310>
- Kusnerik, K. M., Lockwood, R., & Grant, A. N. (2018). Using the fossil record to establish a baseline and recommendations for oyster mitigation in the Mid-Atlantic U.S. In C. L. Tyler & C. L. Schneider (Eds.), *Marine Conservation Paleobiology* (pp. 75–103). Springer International Publishing. https://doi.org/10.1007/978-3-319-73795-9_5
- Laslett, G. M., Eveson, J. P., & Polacheck, T. (2004). Fitting growth models to length frequency data. *ICES Journal of Marine Science*, 61(2), 218–230. <https://doi.org/10.1016/j.icesjms.2003.12.006>
- Lemasson, A. J., Fletcher, S., Hall-Spencer, J. M., & Knights, A. M. (2017). Linking the biological impacts of ocean acidification on oysters to changes in ecosystem services: A review. *Journal of Experimental Marine Biology and Ecology*, 492, 49–62. <https://doi.org/10.1016/j.jembe.2017.01.019>
- Macdonald, P. D. M., & Pitcher, T. J. (1979). Age-Groups from Size-Frequency Data: A Versatile and Efficient Method of Analyzing Distribution Mixtures. *Journal of the Fisheries Research Board of Canada*, 36(8), 987–1001. <https://doi.org/10.1139/f79-137>
- Mann, R., & Powell, E. N. (2007). Why oyster restoration goals in the Chesapeake Bay are not and probably cannot be achieved. *Journal of Shellfish Research*, 26(4), 905–917. [https://doi.org/10.2983/0730-8000\(2007\)26%5B905:WORGIT%5D2.0.CO;2](https://doi.org/10.2983/0730-8000(2007)26%5B905:WORGIT%5D2.0.CO;2)
- Mann, R., Southworth, M., Harding, J. M., & Wesson, J. A. (2009). Population studies of the native eastern oyster, *Crassostrea Virginica*, (Gmelin, 1791) in the James river, Virginia, USA. *Journal of Shellfish Research*, 28(2), 193–220. <https://doi.org/10.2983/035.028.0203>
- Mann, R., Southworth, M., Wesson, J., Thomas, J., Tarnowski, M., & Homer, M. (2022). Oyster shell production and loss in the Chesapeake Bay. *Journal of Shellfish Research*, 40(3). <https://doi.org/10.2983/035.040.0302>
- Marquardt, A. R., Southworth, M., & Mann, R. (2024). Oyster allometry: Growth relationships vary across space. *Journal of the Marine Biological Association of the United Kingdom*, 104, e119. <https://doi.org/10.1017/S0025315424001140>
- Mildenberger, T. K., Taylor, M. H., & Wolff, M. (2017). **TropFishR**: An R package for fisheries analysis with length-frequency data. *Methods in Ecology and Evolution*, 8(11), 1520–1527. <https://doi.org/10.1111/2041-210X.12791>
- National Academies of Science, Engineering, and Medicine. (2019). *A decision framework for interventions to increase the persistence and resilience of coral reefs* (p. 198). The National Academies Press. <https://doi.org/10.17226/25424>
- Neath, A. A., & Cavanaugh, J. E. (2012). The Bayesian information criterion:

- Background, derivation, and applications. *WIREs Computational Statistics*, 4(2), 199–203. <https://doi.org/10.1002/wics.199>
- Pace, S. M., Poussard, L. M., Powell, E. N., Ashton-Alcox, K. A., Kuykendall, K. M., Solinger, L. K., Hemeon, K. M., & Soniat, T. M. (2020). Dying, decaying, and dissolving into irrelevance: First direct in-the-field estimate of *Crassostrea Virginica* Shell Loss—a Case History from Mississippi Sound. *Journal of Shellfish Research*, 39(2), 245. <https://doi.org/10.2983/035.039.0206>
- Powell, E. N., Klinck, J., Ashton-Alcox, K., Hofmann, E., & Morson, J. (2012). The rise and fall of *Crassostrea Virginica* oyster reefs: The role of disease and fishing in their demise and a vignette on their management. *Journal of Marine Research*, 70(2-3). <https://doi.org/10.1357/002224012802851878>
- Powell, E. N., Kraeuter, J. N., & Ashton-Alcox, K. A. (2006). How long does oyster shell last on an oyster reef? *Estuarine, Coastal and Shelf Science*, 69(3-4), 531–542. <https://doi.org/10.1016/j.ecss.2006.05.014>
- Pritchard, D. (1952). Salinity distribution and circulation in the Chesapeake Bay estuarine system. *Journal of Marine Research*, 11(2).
- Ross, P. M., Pine, C., Scanes, E., Byrne, M., O'Connor, W. A., Gibbs, M., & Parker, L. M. (2024). Meta-analyses reveal climate change impacts on an ecologically and economically significant oyster in Australia. *iScience*, 27(12). <https://doi.org/10.1016/j.isci.2024.110673>
- Rutter, C. (1902). Natural history of the Quinnet salmon: A report of investigations in the Sacramento River 1896-1901. *Bulletin United States Fish Commission*, 22, 65–141.
- Rybovich, M., Peyre, M. K. L., Hall, S. G., & Peyre, J. F. L. (2016). Increased Temperatures Combined with Lowered Salinities Differentially Impact Oyster Size Class Growth and Mortality. *Journal of Shellfish Research*, 35(1), 101–113. <https://doi.org/10.2983/035.035.0112>
- Schulte, D. M. (2017). History of the Virginia oyster fishery, Chesapeake Bay, USA. *Frontiers in Marine Science*, 4.
- Scrucca, L., Fraley, C., Murphy, T. B., & Raftery, A. E. (2023). *Model-Based Clustering, Classification, and Density Estimation Using mclust in R* (1st ed.). Chapman and Hall/CRC. <https://doi.org/10.1201/9781003277965>
- Sethi, S. A., Gerken, J., & Ashline, J. (2017). Accurate aging of juvenile salmonids using fork lengths. *Fisheries Research*, 185, 161–168. <https://doi.org/10.1016/j.fishres.2016.09.012>
- Shaw, C. T., Bi, H., Feinberg, L. R., & Peterson, W. T. (2021). Cohort analysis of *Euphausia Pacifica* from the Northeast Pacific population using a Gaussian mixture model. *Progress in Oceanography*, 191, 102495. <https://doi.org/10.1016/j.pocean.2020.102495>
- Solinger, L. K., Ashton-Alcox, K. A., Powell, E. N., Hemeon, K. M., Pace, S. M., Soniat, T. M., & Poussard, L. M. (2022). Oysters beget shell and vice versa: Generating management goals for live oysters and the associated reef to promote maximum sustainable yield of *Crassostrea Virginica*. *Canadian Journal of Fisheries and Aquatic Sciences*, 79(8), 1241–1254. <https://doi.org/10.1139/cjfas-2021-0277>

- Southworth, M., Harding, J. M., Wesson, J. A., & Mann, R. (2010). Oyster (*Crassostrea Virginica*, Gmelin 1791) Population Dynamics on Public Reefs in the Great Wicomico River, Virginia, USA. *Journal of Shellfish Research*, 29(2), 271–290. <https://doi.org/10.2983/035.029.0202>
- Stephens, M. (2000). Bayesian Analysis of Mixture Models with an Unknown Number of Components- An Alternative to Reversible Jump Methods. *The Annals of Statistics*, 28(1), 40–74. <https://www.jstor.org/stable/2673981>
- von Bertalanffy, L. (1938). *A quantitative theory of organic growth (inquiries on growth laws II)*. 10, 181–213. <https://www.jstor.org/stable/41447359>
- Waldbusser, G. G., Steenson, R. A., & Green, M. A. (2011). Oyster Shell Dissolution Rates in Estuarine Waters: Effects of pH and Shell Legacy. *Journal of Shellfish Research*, 30(3), 659–669. <https://doi.org/10.2983/035.030.0308>
- Weise, E. M., Scribner, K. T., Adams, J. V., Boeberitz, O., Jubar, A. K., Bravener, G., Johnson, N. S., & Robinson, J. D. (2022). Pedigree analysis and estimates of effective breeding size characterize sea lamprey reproductive biology. *Evolutionary Applications*, 15(3), 484–500. <https://doi.org/10.1111/eva.13364>
- Zhou, S., Martin, S., Fu, D., & Sharma, R. (2020). A Bayesian hierarchical approach to estimate growth parameters from length data of narrow spread. *ICES Journal of Marine Science*, 77(2), 613–623. <https://doi.org/10.1093/icesjms/fsz241>